Shape-Controlled Anatase Titanium(IV) Oxide Particles Prepared by Hydrothermal Treatment of Peroxo Titanic Acid in the Presence of Polyvinyl Alcohol

Shape-controlled anatase titanium(IV) oxide particles prepared by hydrothermal treatment of peroxo titanic acid in the presence of polyvinyl alcohol

*Naoya Murakami, Yu Kurihara, Toshiki Tsubota and Teruhisa Ohno**

Department of Applied Chemistry, Faculty of Engineering, Kyushu Institute of Technology, 1-1 Sensuicho, Tobata, Kitakyushu 804-8550, Japan

AUTHOR EMAIL ADRESS: murakami@che.kyutech.ac.jp

* CORRESPONDING AUTHOR: Teruhisa Ohno

TEL & FAX: +81-93-884-3318, EMAIL ADRESS: tohno@che.kyutech.ac.jp

ABSTRACT

Anatase titanium(IV) oxide (TiO_2) particles with specific exposed crystal faces were prepared by hydrothermal treatment of peroxo titanic acid (PTA) solution with polyvinyl alcohol as a shape-control reagent. Crystal phase, shape and size of TiO_2 particles were found to be greatly dependent on pH value of PTA solution and time of hydrothermal treatment. TiO_2 particles prepared from PTA solution of pH 7 had {101} and {001} exposed-crystal-face, and the shape of TiO_2 particles changed with the time of hydrothermal treatment. The prepared TiO_2 particles with specific exposed crystal faces showed higher photocatalytic activity for acetaldehyde decomposition than commercial spherical TiO_2 particles. This result implies that back reaction was prevented by spatial separation of redox sites in the particles

because of selective migration of electrons and positive holes to specific exposed crystal faces and/or different reactivity of electrons and positive holes on the specific exposed crystal face. Furthermore, the shape evolution of TiO_2 particles showed a relationship with photocatalytic activity, and a stacked structure of octahedral anatase showed the highest photocatalytic activity due to both oxidation and reduction sites with large surface area.

1. Introduction

Semiconductor particles are attractive material as a photocatalyst because of the large number of surface reaction sites, and semiconductor particles with large surface area have been utilized for various kinds of photocatalytic reaction, such as organic decomposition and water splitting.[1-4] Photocatalytic reaction over semiconductor particles is caused by excited electrons and positive holes, which migrate in the bulk and induce reduction and oxidation, respectively, by reacting with adsorbed species on the surface. However, both of the reactions proceed in neighboring sites on the same particle, and back reaction (including recombination) easily occurs, resulting in decline of photocatalytic efficiency. The back reaction is more likely to occur in the case of small particles because electrons and positive holes cannot be sufficiently separated from each other in the limited spatial region. Therefore, reduction of crystal size sometimes decreases photocatalytic activity due to increase in back reaction as well as decrease in crystallinity, which is correlated with recombination rate and is also a determinant factor of photocatalytic activity.

Physical chemical properties of particles are dependent on both the bulk and surface properties, but the photochemical property for interfacial reactions, e.g., heterogeneous photocatalytic reaction, will be dominated by the surface properties rather than the bulk ones as the particle size decreases. Therefore, control of surface structure is one possible method for improving efficiency of interfacial reaction on a semiconductor nanoparticle. In our previous study, we utilized the geometrical structure of a titania nanotube and developed a novel photocatalyst by site-selective deposition of platinum (Pt) particles

inside/outside the nanotube.[5] The photocatalyst showed a higher photocatalytic activity than conventional spherical particles and a titania nanotube with non-selective deposition of Pt because of the spatial separation of redox sites due to site-selective deposition of Pt particles. However, an expensive Pt cocatalyst is necessary for this method because efficient spatial separation of redox sites does not occur on pristine titania nanotube.

It has been reported that titanium(IV) oxide (TiO_2) particles with specific exposed crystal faces, i.e., octahedral anatase with {101} and {001} exposed crystal face and dodecahedral rutile with {110} and {101} exposed crystal faces, showed excellent photocatalytic activity despite the large particle size (~1 μm).[6] That study indicated that different energy levels of conduction and valence bands, which are determined by the arrangement and kind of constituent atoms, drive the electrons and positive holes to different exposed crystal faces, resulting in a decrease in the back-reaction rate by predominant progress of reduction and oxidation on each crystal face. Optical, magnetic, dielectric and chemical properties of a particle are thought to depend on the shape of the crystal particle,[7-10] and an electrode experiment using single-crystal rutile TiO_2 has indicated that photoelectrochemical properties also depend on the kind of exposed crystal face.[11-13] The results of those studies suggest that it is possible to optimize activity of a specific photocatalytic reaction by controlling the kind and surface area of the exposed crystal face on semiconductor particles.

Several groups have reported method for preparing TiO_2 particles with specific exposed crystal faces using organic and inorganic reagents,[14-24] and further control of the exposed crystal face by a chemical etching method.[25] However, there have been few reports in which the relationship between surface structure and photocatalytic activity was described.[25,26] One of the reasons for this is that some shape-control reagents cause deterioration of photocatalytic activity by strong adsorption on the surface or being doped into the lattice, though they induce the formation of a well-defined crystal face with a single crystal phase. Recently, hydrophilic polymers, such as polyvinyl alcohol (PVA) and polyvinylpyrrolidone (PVP), have been used as shape-control reagents of metal and metal oxide particles.[27-29] PVA is a well-known nontoxic hydrophilic polymer and can be removed by photocatalytic

decomposition.[30] In the present study, anatase TiO_2 particles with specific exposed crystal faces were prepared by hydrothermal treatment using PVA as a shape-control reagent. Physical chemical properties of the particles prepared by a PVA-assisted hydrothermal method, which was developed from a previously reported method,[28] were studied with focus on morphology and surface structure, and relationships of their characteristic features with photocatalytic activity for acetaldehyde decomposition were examined.

2. Experimental

2.1 Sample preparation

0.5 cm^3 of mili-Q water was added to 1 cm^3 of titanium(IV) ethoxide and 30 cm^3 of ethanol with vigorous stirring, and the mixture was stirred for 30 min at room temperature. The resulting precipitate was centrifugally separated from the solution and dried under reduced pressure. One mg of obtained titanium hydroxide particles was dispersed in 50 cm^3 of mili-Q water and then irradiated by ultrasonication. Thirty two cm^3 of 30% hydrogen peroxide was added and yellow peroxo titanic acid (PTA) solution was obtained, and then ammonium (NH_3) solution as a pH-adjusting agent and PVA (M_w = 22000) as a shape-control reagent were added to the solution. After stirring the solution at ca. 60 ^oC for 24 h, the solution in a Teflon bottle sealed with a stainless jacket was heated at 200 ^oC for 3-48 h in an oven. After the hydrothermal treatment, the residue in the Teflon bottle was washed with acetone, ethanol and mili-Q water several times and organic compounds on the TiO_2 particles were removed by 24 h of ultraviolet (UV) irradiation with a 500-W super-high-pressure mercury lamp (Ushio, SX-UI501UO), light intensity of which was 600 mW cm^{-2}. The particles were dried under reduced pressure at 60 °C for 12 h.

2.2 Characterization

The crystal structures of TiO_2 particles were determined from X-ray diffraction patterns measured with an X-ray diffractometer (JEOL, JDX3500) with a Cu target Kα-ray (λ = 1.5405 Å). The specific

surface areas of the particles (S_{BET}) were determined with a surface area analyzer (Quantachrome, Autosorb-1) by using the Brunauer-Emmett-Teller (BET) equation. The morphology of prepared TiO_2 particles was observed by using a transmission electron microscope (TEM; Hitachi, H-9000NAR) and a scanning electron microscope (SEM; JEOL, JSM-6701FONO).

2.3 Photocatalytic decomposition of acetaldehyde

Photocatalytic activity of TiO_2 samples was evaluated by photocatalytic decomposition of acetaldehyde. One hundred mg of TiO_2 particles was spread on a glass dish, and the glass dish was placed in a Tedlar bag (AS ONE Co. Ltd.) with a volume of 125 cm^3. Five hundred ppm of gaseous acetaldehyde was injected into the Tedlar bag, and photoirradiation was carried out at room temperature after acetaldehyde had reached an adsorption equilibrium. The gaseous composition in Tedlar bag were 79 % of N_2, 21 % of O_2, < 0.1 ppm of CO_2 and 500 ppm of acetaldehyde, and relative humidity was ca. 30 %. A 500-W xenon lamp (Ushio, SX-UI501XQ) was used as a light source and the wavelength of photoirradiation was controlled by a UV-35 filter (Asahi Techno Glass). Intensity of the light was adjusted to 12 mW cm^{-2}. Concentrations of acetaldehyde and carbon dioxide (CO_2) were estimated by gas chromatography (Shimadzu, GC-8A, FID detector) with an PEG-20 M 20% Celite 545 packed glass column and by gas chromatography (Shimadzu, GC-9A, FID detector) with a TCP 20% Uniport R packed column and methanizer (GL Sciences, MT-221), respectively. In photocatalytic evaluation, P-25 (Japan Aerosil, S_{BET} = 50 m^2 g^{-1}), which is a well-known commercial TiO_2 photocatalyst with high photocatalytic activity, was evaluated as a standard photocatalyst. Before the evaluation, all of TiO_2 samples were pretreated by UV irradiation with a black light in order to remove contaminant on TiO_2 surface, and all of photocatalytic evaluation was carried out under same experimental condition, such as temperature, acetaldehyde concentration, air relative humidity and incident light intensity.

2.4 Photodeposition of Pt and lead(IV) oxide (PbO_2) on TiO_2 particles

In order to determine reduction and oxidation sites on TiO_2 particles, photodeposition of Pt and PbO_2 was carried out, respectively.[6,31] For determination of reduction sites, an aqueous suspension composed of TiO_2 particles and an isopropyl alcohol solution (10 vol%) containing 1 mmol dm^{-3} of hexachloroplatinic acid ($H_2PtCl_6 \cdot 6H_2O$) was photoirradiated with a mercury lamp (5 mW cm^{-2}) under an argon atmosphere with vigorous magnetic stirring. For determination of oxidation sites, an aqueous suspension composed of TiO_2 particles and 1 mmol dm^{-3} of lead(II) nitrate ($Pb(NO_3)_2$) solution was photoirradiated with a mercury lamp (300 mW cm^{-2}) under an aerated atmosphere with vigorous magnetic stirring. After irradiation, photodeposited samples were obtained by washing with water several times and drying.

3. Results and discussion

3.1 Effect of pH of PTA solution without PVA

Crystal phase and shape of prepared TiO_2 particles were greatly influenced by pH of the PTA solution, though S_{BET} of the TiO_2 particles showed slight dependence on pH (78 m^2 g^{-1} for pH 4, 69 m^2 g^{-1} for pH 7 and 68 m^2 g^{-1} for pH 10). Figure 1 shows XRD patterns of TiO_2 particles prepared by 3 h of hydrothermal treatment of PTA solutions of pH 4, 7 and 10 without PVA. The prepared TiO_2 was a mixture of anatase and rutile phases, and the anatase phase increased with increase in pH, while rutile phase decreased.

Figure 2 shows primary particle size (d) estimated from the XRD patterns using the Scherrer equation ($d = 0.9\lambda/\beta\cos\theta_B$, where λ is wavelength of X-ray, β is full width at half maximum and θ_B is Bragg angle). The β was estimated by fitting the XRD patterns with a superposition of Lorentz functions for peaks attributed to anatase and rutile. Anatase particle size along the [001] direction estimated by a peak attributed to (004) of anatase TiO_2 ($d_{A(004)}$) increased with increase in pH of the PTA solution, while rutile particle size along the [001] direction estimated by a peak attributed to (002) of rutile TiO_2 ($d_{R(002)}$) decreased. On the other hand, anatase particle size along the [100] direction ($d_{A(200)}$) and rutile particle size along the [110] direction ($d_{R(110)}$), which were estimated from peaks attributed to (200) of

anatase and (110) of rutile TiO_2 respectively, showed almost constant values regardless of the pH value. Although large error bars of $d_{R(002)}$ suggest that it is difficult to estimate an accurate value of $d_{R(002)}$ using the Scherrer equation due to superposition of peaks attributed to (204) of anatase and (002) of rutile, tendency that $d_{R(002)}$ decrease with increase in pH of the PTA solution can be observed.

Figure 3 shows TEM images of TiO_2 particles prepared without PVA. The TiO_2 sample prepared from the solution of pH 4 was mixture of rod-like structures with an aspect ratio of ca. 4 and fine particles that were aggregated and attached to the larger particles (Fig. 3a). Most of the rods consisted of flat side surfaces and triangular-like caps, similar to the structure reported for rutile rods with {110} and {111} exposed crystal faces and longer length along the [001] direction.[21,22] The aspect ratio of primary particle size estimated from XRD analysis (Fig. 2), i.e., $d_{R(002)}/d_{R(110)} \sim 3$, $d_{A(004)}/d_{A(200)} \sim 1$, strongly suggests that rutile rods and anatase spheres were formed under an acidic condition. Under a neutral condition (pH 7), another kind of rod with a stepped side surface was also formed in addition to the above-mentioned rutile rods (Fig. 3b). The aspect ratio of primary particle size suggests that the rod is attributed to anatase TiO_2 that has grown along the [001] direction because $d_{A(004)}/d_{A(200)}$ is ca. 2.4. Under a basic condition (pH 10), aggregated particles with different sizes were observed in a TEM image (Fig. 3c), and XRD analysis indicated that the TiO_2 particles prepared at pH 10 consisted of large anatase particles and small rutile particles, and size of the anatase particle was similar to that of anatase in the TiO_2 particles prepared at pH 7.

These results suggest that crystal phase and shape were influenced by pH; i.e., rutile rods with flat surfaces were formed under an acidic condition, while anatase rods with stepped surfaces were formed under a basic condition. It has been reported that the structure of a titanium complex, which is changed by the pH of solution, has an influence on crystal phase, shape and size,[14,32] and anatase rods similar to those shown in Fig. 3b were prepared from PTA solution by using sodium hydroxide (NaOH) solution as a pH-adjusting agent.[33] Results of those studies strongly suggest that not NH_3 but pH of the solution is important for the formation of crystal phase, shape and size. For preparation of a TiO_2 photocatalyst, NH_3 solution is thought to be preferable as a pH-adjusting agent rather than NaOH because sodium ions

sometime remains in the TiO_2 lattice and reduce the photocatalytic activity. Some studies have suggested that addition of NH_3 solution to a precursor solution causes nitrogen doping,[34] which induces color change of TiO_2 from white to yellow. However, the obtained TiO_2 particles were almost white in color, suggesting absence of nitrogen doping in TiO_2.

3.2 Effect of pH of PTA solution with PVA

Figure 4 shows XRD patterns of TiO_2 particles prepared by 3 h of hydrothermal treatment of PTA solutions of pH 4, 7 and 10 with 50 mg of PVA. Crystal phase of the TiO_2 particles was only anatase structure regardless of pH of the PTA solution, suggesting that PVA prevented the nucleation of rutile phase. On the other hand, the size of TiO_2 particles was greatly influenced by pH of the PTA solution, and the pH dependence of $d_{A(004)}$ of prepared TiO_2 with PVA was similar as that of TiO_2 without PVA; i.e., $d_{A(004)}$ increased at pH < 7 and became saturated at pH > 7 (Figure 5).

Figure 6 shows TEM images of TiO_2 particles. The TiO_2 particles prepared from the solution of pH 4 were fine particles of ca. 10 nm in diameter (Fig. 6a). In a TEM image of TiO_2 samples prepared from PTA solution of pH 7 (Fig. 6b), polyhedral projections, such as square-like projection of a ca. 30-nm particle, were observed. This polyhedral projection indicates that the particle had a specific exposed crystal face, and the plausible structure of the square-shaped projection is perhaps attributed to decahedral anatase TiO_2 with {101} and {001} exposed crystal faces, which are the two most stable crystal faces of anatase.[35] Although similar TiO_2 particles were formed under a basic condition, particles with rough surfaces and aggregated fine particles on larger particles were observed, indicating that higher pH caused failure of control of a well-defined crystal face. On the other hand, fine particles with a narrow size distribution that were prepared under an acidic condition, suggest that PVA may lead a prevention of aggregation and a formation of a flat exposed surface by adsorption on TiO_2 in the crystallization process.

Even in the presence of PVA, addition of NH_3 solution had an influence on shape control as a result of coordination to PTA and/or pH control of the PTA solution. Kakihana et al. reported stable titanium

complexes prepared by coordination of NH_3 and organic acid to PTA, and they prepared shape-controlled TiO_2 particles by utilizing the stable nature in hydrothermal preparation.[16-20,36] However, in our study, excess addition of NH_3 solution induced the formation of a poorly defined crystal face, presumably implying that NH_3 worked as a pH-adjusting agent rather than the above-mentioned stabilizer of a titanium complex.

Sugimoto et al. reported that adsorption of amine on titanium hydroxide gel showed dependence on pH of the solution, causing changes in the crystal phase, shape and size.[14,15] Calculations[37-39] and results of another experimental study[40] indicated that surface properties also depend on the specific crystal planes. Therefore, the formation of a {101} exposed crystal face can be explained by the adsorption properties of PVA, which depended on both the exposed crystal face and pH of the solution.

3.3 Shape evolution of TiO_2 particles with increase in time of hydrothermal treatment

Prepared TiO_2 particles showed shape evolutions with increase of time in hydrothermal treatment. Figure 7 shows XRD patterns of TiO_2 particles prepared by 3-48 h of hydrothermal treatment of PTA solution of pH 7 with 30 mg of PVA. All the prepared TiO_2 particles showed similar XRD patterns attributed to pure anatase, and length along the [001] direction ($d_{A(004)}$) showed dependence on the time of hydrothermal treatment (Figure 8). The value of $d_{A(004)}$ decreased up to 12 h and then increased after 12 h, while the diameter ($d_{A(200)}$) hardly changed. These results agree with TEM observation of the prepared TiO_2 particles (Figure 9). For the TiO_2 sample prepared by 3 h of hydrothermal treatment, two kinds of anatase particles (Fig. 9a), high-aspect-ratio rods with flat side surfaces (Fig. 9e) and low-aspect-ratio rods with stepped side surfaces (Fig. 9f), were observed. Similar rods with stepped side surfaces were also observed for TiO_2 prepared without PVA (Fig. 3b), though TiO_2 prepared with PVA possess a {001} exposed crystal face and smaller length along the [001] direction. In TEM images of TiO_2 prepared by >12 h of hydrothermal treatment (Fig. 9b-d), square and diamond-like projections were mainly observed, suggesting the formation of decahedral anatase with small and large $d_{A(004)}$, respectively. Figure 10 shows TEM image and selected-area electron diffraction (SAED) pattern of

TiO_2 prepared by 48 h of hydrothermal treatment with 30 mg of PVA. TEM image and SAED pattern indicated that the TiO_2 particle was decahedral shape with {001} and {101} exposed crystal faces. The TEM image also indicates that one of exposed crystal faces is attributed to {101} plane because angles between (101) and (10-1) planes are calculated to be 136.5°.

A plausible mechanism of shape evolution of anatase particles (Figure 11) is as follows: (1) formation of anatase rods having a stacked structure with decahedral anatase with {101} and {001} crystal faces and growth in the [001] direction, (2) transformation of anatase rods into octahedral anatase by size reduction along the [001] direction[41] or by being split along the {001} plane in the dissolution process,[42] and (3) growth of anatase particle in the [001] direction with exposure of the {101} crystal face and evolution of decahedral anatase with large $d_{A(004)}$ in the recrystallization process.

3.4 Effect of amount of PVA (T = 3 h, pH 7)

XRD and TEM results suggest that a large amount of PVA induces the formation of a large fraction of anatase TiO_2 particles with specific exposed crystal faces. Although TiO_2 particles prepared with 10 mg of PVA contained an appreciable amount of rutile (data not shown), a slight difference between surface structures of TiO_2 prepared with 30 and 50 mg was observed. This means that addition of 30 mg of PVA was sufficient to prepare anatase TiO_2 particles with specific exposed crystal faces. Addition of an excess amount of PVA sometimes caused deterioration of photocatalytic activity. This will be discussed in later section (Section 3.5.2).

3.5 Evaluation of photocatalytic activity for acetaldehyde decomposition

3.5.1 Effect of pH of PTA (T = 3 h, PVA = 50 mg)

Photocatalytic activity for acetaldehyde decomposition strongly depended on the surface structure of prepared TiO_2 particles. Figure 12 shows the time course of CO_2 evolution over TiO_2 particles prepared by 3 h of hydrothermal treatment of PTA solutions of pH 4, 7 and 10 with 50 mg of PVA. TiO_2 particles prepared at pH 7, which had specific exposed crystal faces, showed a higher photocatalytic

activity ((b) pH 7 > (a) pH 4 > (c) pH 10) despite having the smallest S_{BET} among these TiO_2 samples (175 m^2 g^{-1} for pH 4, 75 m^2 g^{-1} for pH 7, 133 m^2 g^{-1} for pH 10), indicating that photocatalytic activity was not determined by S_{BET} but by another factor. A plausible candidate is surface structure; the specific exposed crystal face observed in TEM images (Fig. 6b) induced separation of redox sites, resulting in enhancement of photocatalytic activity.[6] Although TiO_2 particles prepared under an acidic condition also seem to have specific exposed crystal faces (Fig. 6a), the activity of the particles was not so high. This result implies that electrons and positive holes in small TiO_2 particles (ca. 10 nm) could not be separated sufficiently for spatial separation of redox sites against coulomb attraction.

3.5.2 Effect of amount of PVA (T = 3 h, pH 7)

Figure 13 shows the time course of CO_2 evolution over TiO_2 particles prepared with various amounts of PVA. Photocatalytic activity of the TiO_2 particles also showed dependence on amount of PVA ((b) 30 mg > (c) 50 mg > (a) without PVA), though S_{BET} showed no dependence on amount of PVA (69 m^2 g^{-1} for without PVA, 67 m^2 g^{-1} for 30 mg and 75 m^2 g^{-1} for 50 mg). TiO_2 prepared with 30 mg of PVA showed a higher photocatalytic activity than TiO_2 without PVA due to the controlled surface structure of TiO_2, as analogy with previous section. However, TiO_2 prepared with 50 mg of PVA showed a lower photocatalytic activity than TiO_2 prepared with 30 mg of PVA in spite of similar surface structures. A possible reason for this is that residual PVA adsorbed on the TiO_2, which was not presumably completely removed by UV irradiation in the preparation procedure, might obstruct photoabsorption and adsorption of reactants, resulting in decrease in efficient photocatalytic reaction. However, CO_2 did not evolved over the TiO_2 samples in the absence of acetaldehyde, suggesting that contaminant of organic compound attributed to PVA did not contribute to CO_2 evolution.

3.5.3 Effect of time of hydrothermal treatment (PVA = 30 mg, pH 7)

Figure 14 shows the time course of CO_2 evolution over TiO_2 particles prepared by various time of hydrothermal treatment. Photocatalytic activity of the prepared TiO_2 particles showed an appreciable

difference depending on the time of hydrothermal treatment ((a) 3 h > (d) 48 h > (c) 24 h ~ (e) P-25 > (b) 12 h), though S_{BET} showed only a slight difference (67 m^2 g^{-1} for 3 h, 77 m^2 g^{-1} for 12 h, 69 m^2 g^{-1} for 24 h, 57 m^2 g^{-1} for 48 h). This presumably implies that photocatalytic activity was influenced by not adsorption properties of acetaldehyde on the TiO_2 surface but the surface structure of TiO_2 particles. Moreover, most of the TiO_2 samples showed higher activity than P-25, which has a high photocatalytic activity for acetaldehyde decomposition among commercial TiO_2 particles. The relationship between surface structure and photocatalytic reaction will be discussed in detail in the following section.

3.6 Photodeposition of Pt and PbO_2 for determination of reduction and oxidation sites

In order to determine the sites on which reduction or oxidation predominantly proceeds, photodeposition of Pt and PbO_2 was carried out. The color of TiO_2 powders after UV-irradiation in the presence of H_2PtCl_6 and $Pb(NO_3)_2$ aqueous solution changed to gray and brown respectively, suggesting that Pt and PbO_2 were deposited on the TiO_2 surface.[6] Furthermore, the presence of Pt and Pb elements was confirmed by X-ray photoelectron spectroscopic analysis. Figure 15 shows SEM images of Pt- and PbO_2-deposited TiO_2 particles that were prepared by 48 h of hydrothermal treatment with PTA solution. Small particles were observed on the specific exposed face of decahedral TiO_2 particles, though we have no information on elemental composition of them. However, small particles were presumably thought to be Pt or PbO_2 deposited on TiO_2 because they were not observed in the bare sample (Fig. 9g). Pt particles of a few nanometers in size were mainly observed on the {101} face of decahedral anatase, while PbO_2 particles of ca. 10 nm in size were deposited on the {001} face of decahedral anatase. These smaller particles were not observed on TiO_2 particles before the photodeposition procedure (Fig. 9g). These results agree with results of a previous study showing that oxidation and reduction predominantly proceed on {001} and {101} faces of decahedral anatase TiO_2, respectively.[6] Decahedral TiO_2 with small $d_{A(004)}$ (Fig. 16a) has a larger surface area of oxidation sites and smaller surface area of reduction sites, while decahedral TiO_2 with large $d_{A(004)}$ (Fig. 16b) has a smaller surface area of oxidation sites and larger surface area of reduction sites. Thus, a trade-off relation exists between surface area of oxidation

and reduction sites. As described in the previous section, a correlation between photocatalytic activity and surface structure of TiO_2 particles was observed, and photocatalytic activity increased with increase in the ratio of {101} to {001} exposed crystal faces. This result suggests that decahedral anatase with a small surface area of {001} and large surface area of {101} is suitable for photocatalytic decomposition of acetaldehyde. The highest photocatalytic activity of TiO_2 particles prepared by 3 h of hydrothermal treatment was presumably due to the larger surface areas of both reduction and oxidation sites on the stacked structure of decahedral TiO_2 (Fig. 16c).

Another possible reason for the highest activity is that the stepped surface itself induces the separation of redox sites. Kato et al. reported that NiO-loaded lanthanum-doped sodium tantalate ($NaTaO_3$) showed a higher photocatalytic activity for water splitting because the grooved and edge surface induced separation of redox sites.[3] In our experiment, similar anatase rods with the stepped faces were also prepared without PVA, though a {001} exposed face was not observed (Fig. 3b) and their activity was not so high. This indicates that the spatial separation of redox sites requires different kinds of exposed crystal surface, i.e., both {001} and {101} exposed crystal faces.

4. Conclusion

Anatase particles with specific exposed crystal faces were prepared by hydrothermal treatment of PTA solution with PVA under a neutral condition. The shapes of prepared anatase TiO_2 particles, which were divided into three types (octahedral anatase with large $d_{(004)}$ and small $d_{(004)}$, and stacked structure of octahedral anatase) as shown in Fig. 16, can be controlled by changing the time of hydrothermal treatment. Photocatalytic activity of acetaldehyde decomposition showed dependence on not S_{BET} but surface structure of TiO_2 particles, and anatase particles with specific exposed crystal faces showed a high photocatalytic activity due to spatial separation of redox sites. Nanorod particles with stacked octahedral anatase showed the highest photocatalytic activity because efficient separation of redox sites was induced by both oxidation and reduction sites with large surface areas.

Further enhancement of photocatalytic activity would be possible by optimizing the aspect ratio of decahedral anatase or anatase nanorods. Moreover, if the size of TiO_2 particles with specific exposed crystal faces is also controllable, the efficiency of the separation will be increased by taking into account the relationship between particle size and diffusion length of electrons and positive holes.

ACKNOWLEDGEMENT

This work was supported by a grant of Knowledge Cluster Initiative implemented by the Ministry of Education, Culture, Sports, Science and Technology (MEXT) and the New Energy and Industrial Technology Development Organization (NEDO).

FIGURE CAPTIONS

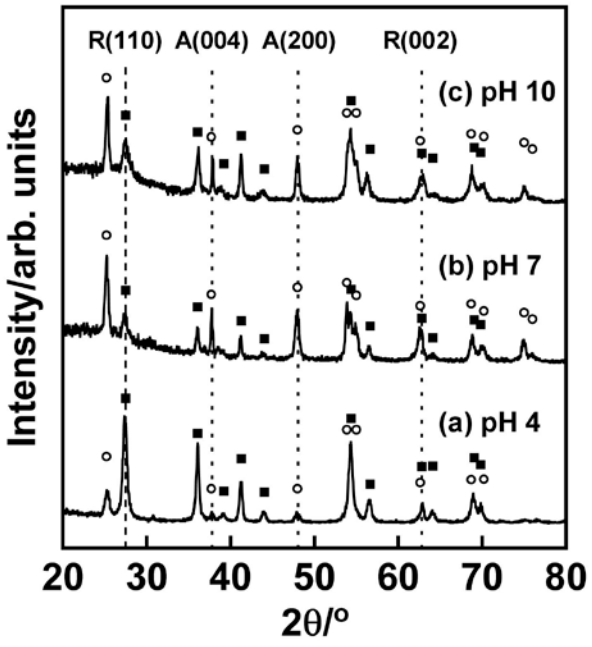

Figure 1. XRD patterns of TiO_2 particles prepared by 3 h of hydrothermal treatment of PTA solution of pH (a) 4, (b) 7 and (c) 10 without PVA (○; anatase, ■; rutile).

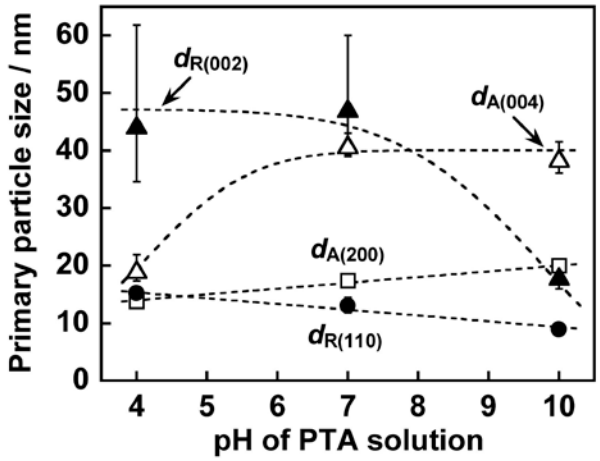

Figure 2. Primary particle size of TiO_2 particles prepared by 3 h of hydrothermal treatment of PTA solution of pH 4, 7 and 10 without PVA.

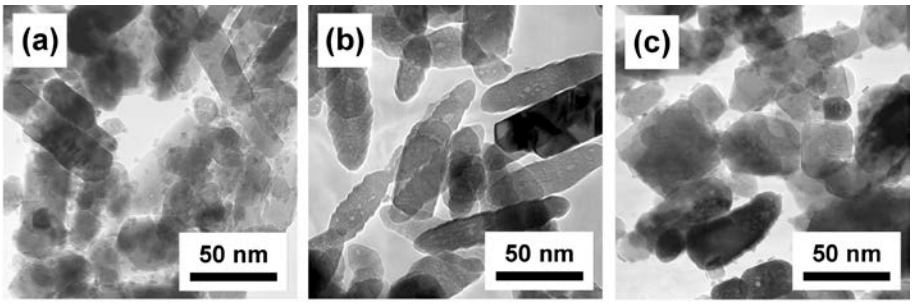

Figure 3. TEM images of TiO_2 particles prepared by 3 h of hydrothermal treatment of PTA solution of pH (a) 4, (b) 7 and (c) 10 without PVA.

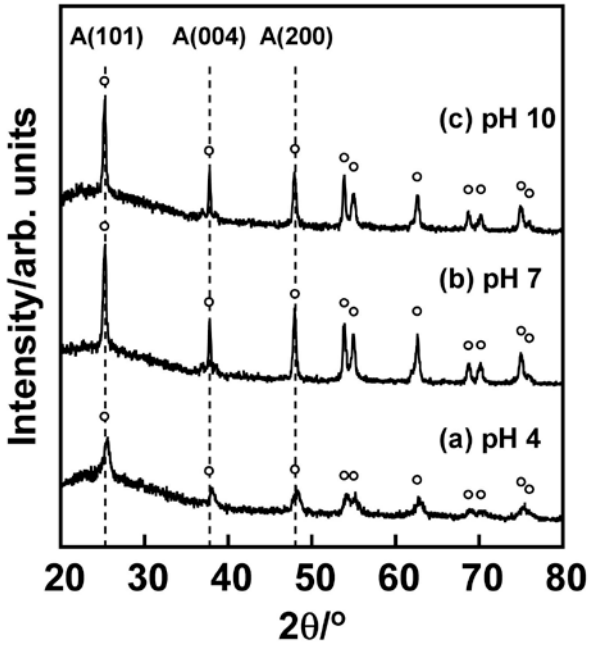

Figure 4. XRD patterns of TiO_2 particles prepared by 3 h of hydrothermal treatment of PTA solution of pH (a) 4, (b) 7 and (c) 10 with 50 mg of PVA (○; anatase).

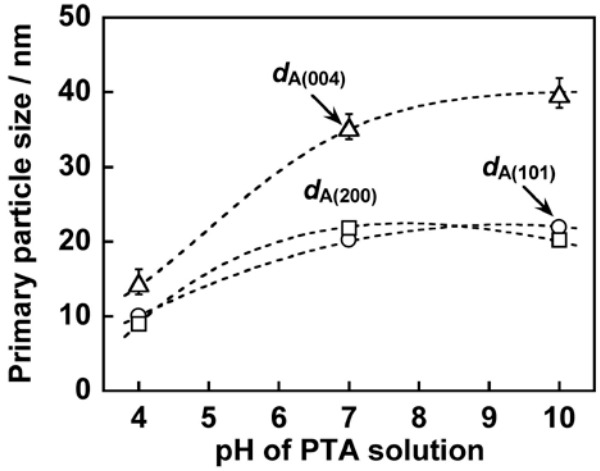

Figure 5. Primary particle size of TiO_2 particles prepared by 3 h of hydrothermal treatment as a function of pH of PTA solution with 50 mg of PVA.

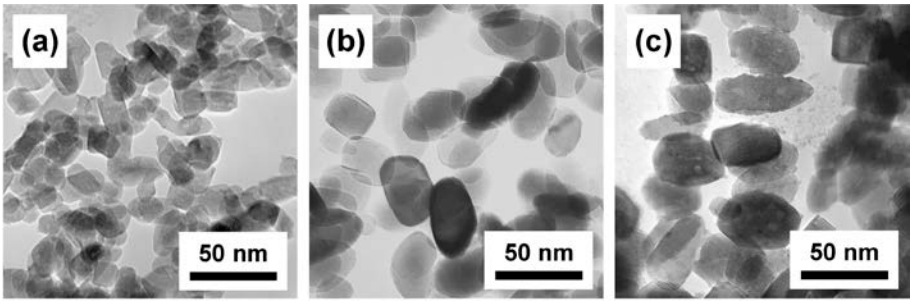

Figure 6. TEM image of TiO_2 particles prepared from PTA solution of pH (a) 4, (b) 7 and (c) 10 with 50 mg of PVA.

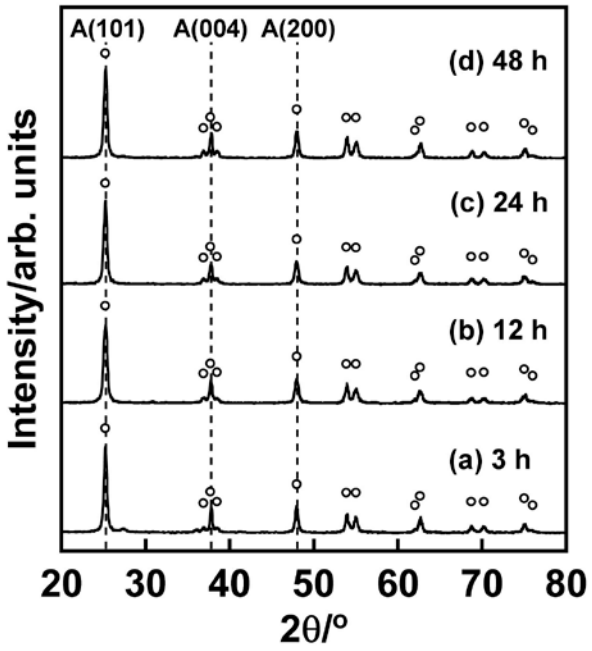

Figure 7. XRD patterns of TiO_2 particles prepared by (a) 3, (b) 12, (c) 24 and (d) 48 h of hydrothermal treatment of PTA solution of pH 7 with 30 mg of PVA (○; anatase).

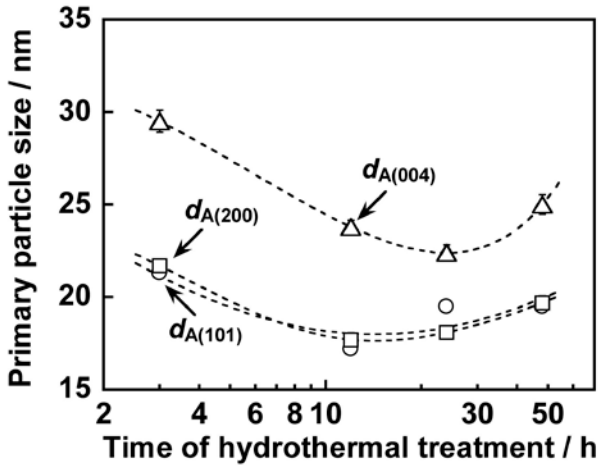

Figure 8. Evolution of primary particle size as a function of time of hydrothermal treatment.

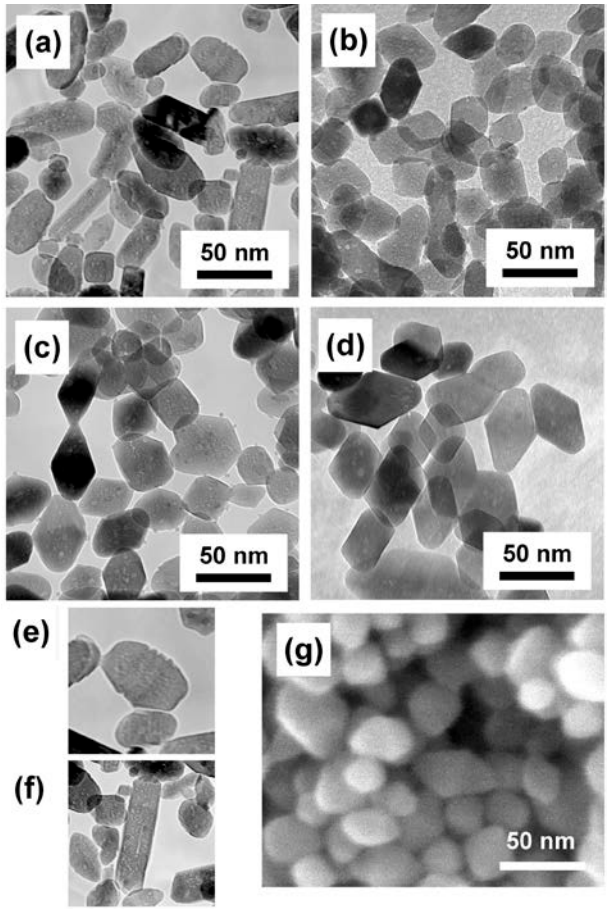

Figure 9. TEM images of TiO_2 particles prepared by (a) 3, (b) 12, (c) 24 and (d) 48 h of hydrothermal treatment of PTA solution of pH 7 with 30 mg of PVA. (e), (f) Two kinds of anatase rod observed in (a). (g) SEM image of TiO_2 particles prepared by 48 h of hydrothermal treatment of PTA solution of pH 7 with 30 mg of PVA.

1

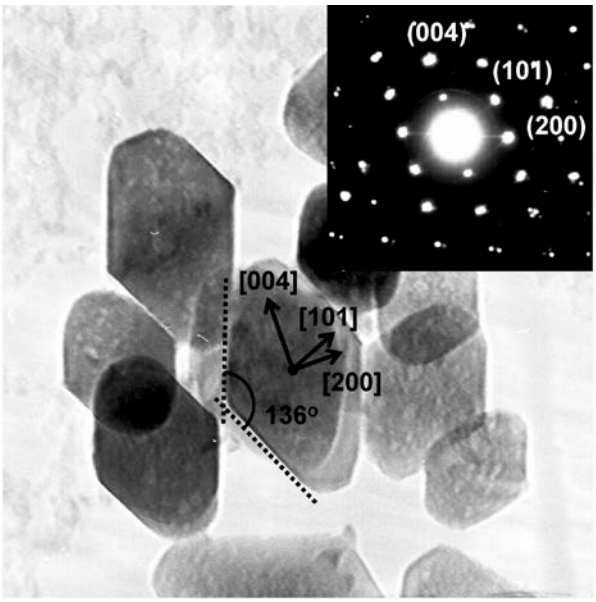

Figure 10. TEM image and SAED pattern of TiO_2 prepared by 48 h of hydrothermal treatment with 30 mg of PVA.

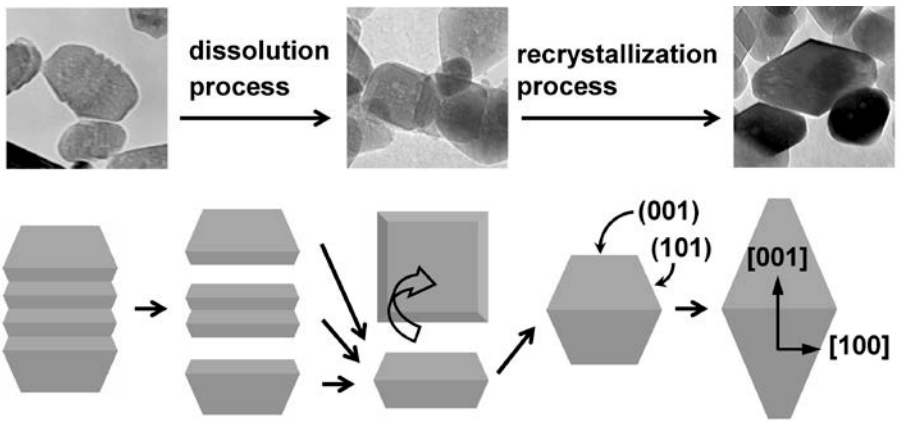

Figure 11. Schematic mechanism of shape evolution of anatase TiO_2 particles in the presence of PVA.

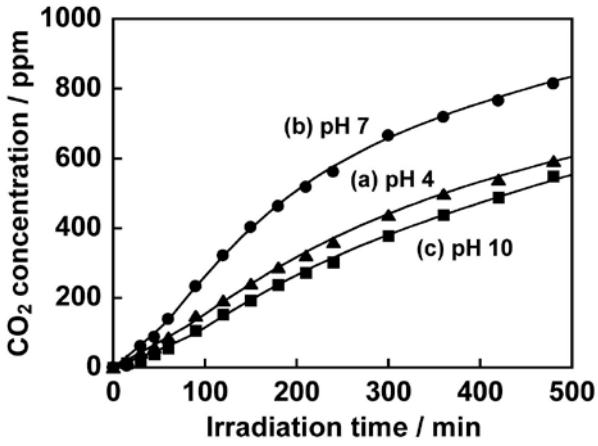

Figure 12. Time course of CO_2 evolution of acetaldehyde decomposition over TiO_2 particles prepared by 3 h of hydrothermal treatment of PTA solution of pH (a) 4, (b) 7 and (c) 10 with 50 mg of PVA.

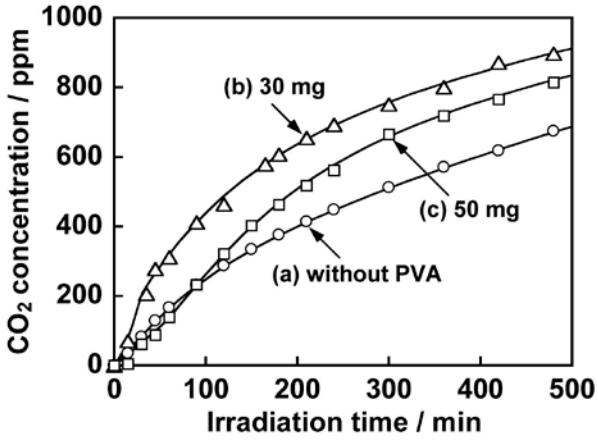

Figure 13. Time course of CO_2 evolution of acetaldehyde decomposition over TiO_2 particles prepared by 3 h of hydrothermal treatment of PTA solution of pH 7 (a) without and with (b) 30 and (c) 50 mg (same data as Fig. 11b) of PVA.

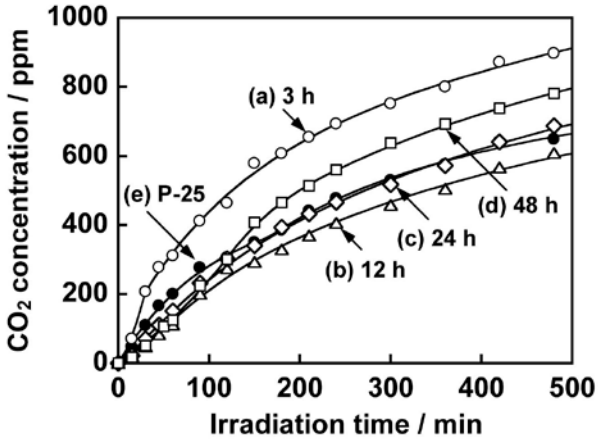

Figure 14. Time course of CO_2 evolution of acetaldehyde decomposition over TiO_2 particles prepared by (a) 3 h (same data as Fig. 12b), (b) 12, (c) 24 and (d) 48 h of hydrothermal treatment of PTA solution of pH 7 with 30 mg of PVA.

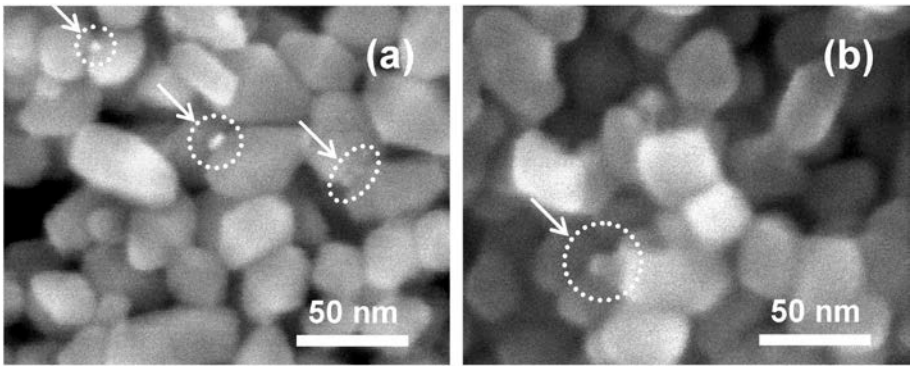

Figure 15. SEM images of (a) Pt-deposited and (b) PbO_2-deposited TiO_2 particles prepared by 48 h of hydrothermal treatment of PTA solution.

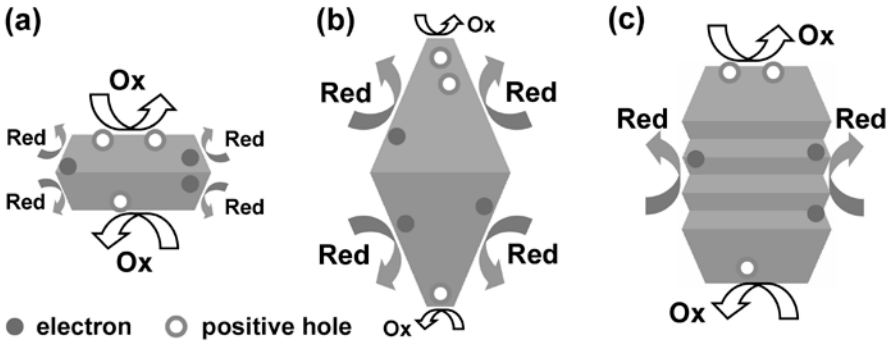

Figure 16. Schematic images of spatial separation of redox sites on anatase TiO_2 particle with specific exposed crystal face. (a) Decahedral particle with a larger surface area of oxidation sites and smaller surface area of reduction sites. (b) Decahedral particle with a smaller surface area of oxidation sites and larger surface area of reduction sites. (c) Stacked-structured particle with larger surface area of both oxidation and reduction sites.

REFERENCES

(1) Hoffmann, M.R.; Martin, S.T.; Choi, W.; Bahnemann, D.W. *Chem. Rev.*, **1995**, *95*, 69.

(2) Fujishima, A.; Rao, T.N.; Tryk, D.A. *J. Photochem. Photobiol. C: Photochem. Reviews,* **2000**, *1*, 79.

(3) Kato, H.; Asakura, K.; Kudo, A. *J. Am. Chem. Soc*., **2003**, *125*, 3082.

(4) Maeda, K.; Teramura, K.; Lu, D.; Takata, T.; Saito, N.; Inoue, Y.; Domen, K. *Nature*, **2006**, *440*, 295.

(5) Nishijima, K.; Fukahori, T.; Murakami, N.; Kamai, T.; Tsubota, T.; Ohno, T. *Appl. Catal. A: Gen.*, **2008**, *337*, 105.

(6) Ohno, T.; Sarukawa, K.; Matsumura, M. *New. J. Chem.*, **2002**, *26*, 1167.

(7) Diebold, U. *Surf. Sci. Rep.*, **2003**, *48*, 53.

(8) Thomas, A.G.; Flavell, W.R.; Kumarasinghe, A.R.; Mallick, A.K.; Tsoutsou, D.; Smith, G.C.; Stockbauer, R.; Patel, S. *Phys. Rev. B*, **2003**, *67*, 035110.

(9) Burda,C.; Chen, X.; Narayanan, R.; El-Sayed, M.A. *Chem. Rev*., **2005**, *105*, 1025.

(10) Dimitrijevic, N.M.; Saponjic, Z.V.; Rabatic, B.M.; Poluektov, O.G.; Rajh, T. *J. Phys. Chem. C*, **2007**, *111*, 14597.

(11) Lowekamp, J. B.; Rohrer, G. S.; Hotsenpiller, P.A.M.; Bolt, J.D.; Farneth, W.E. *J. Phys. Chem. B*, **1998**, *102*, 7323.

(12) Hotsenpiller, P.A.M.; Bolt, J.D.; Farneth, W.; Lowekamp, J.B.; Rohrer G.S. *J. Phys. Chem. B*, **1998**, *102*, 3216.

(13) Imanishi, A.; Suzuki, H.; Murakoshi, K.; Nakato, Y. *J. Phys. Chem. B*, **2006**, *110*, 21050.

(14) Sugimoto, T.; Zhou, X.; Muramatsu, A. *J. Colloid. Interface Sci.*, **2003**, *259*, 43.

(15) Sugimoto, T.; Zhou, X.; Muramatsu, A. *J. Colloid. Interface Sci.*, **2003**, *259*, 53.

(16) Tomita, K.; Petrykin, V.; Kobayashi, M.; Shiro, M.; Yoshimura, M.; Kakihana, M. *Angew. Chem. Int. Ed.*, **2006**, *45*, 2378.

(17) Kobayashi, M.; Petrykin, V.; Kakihana, M.; Tomita, K. *J. Ceram. Soc. Jpn.*, **2007**, *115*, 835.

(18) Kobayashi, M.; Petrykin, V.; Tomita, K.; Kakihana, M. *J. Ceram. Soc. Jpn.*, **2008**, *116*, 578.

(19) Kobayashi, M.; Koji, T.; Petrykin, V.; Yoshimura, M.; Masato, K. *J. Mater. Sci.*, **2008**, *43*, 2159.

(20) Tomita, K.; Kobayashi, M.; Petrykin, V.; Yin, S.; Sato, T.; Yoshimura, M.; Kakihana, M. *J. Mater. Sci.*, **2008**, *43*, 2217.

(21) Hosono, E.; Fujihara, S.; Kakiuchi, K.; Imai, K. *J. Am. Chem. Soc.*, **2004**, *126*, 7790.

(22) Kakiuchi, K.; Hosono, E.; Imai, H.; Kimura, T.; Fujihara, S. *J. Cryst. Growth*, **2006**, *293*, 541.

(23) Yang, H.G.; Sun, C.H.; Qiao, S.Z.; Zou, J.; Liu, G.; Smith, S.C.; Cheng, H.M.; Lu, G.Q. *Nature*, **2008**, *453*, 638.

(24) Jun, Y.; Choi, J.; Cheon, J. *Angew. Chem. Int. Ed.*, **2006**, *45*, 3414.

(25) Taguchi, T.; Saito, Y.; Sarukawa, K.; Ohno, T.; Matsumura, M. *New. J. Chem.*, **2003**, *27*, 1304.

(26) Cho, C.H.; Han, M.H.; Kim, D.H.; Kim, D.K. *Mater. Chem. Phys.*, **2005**, *92*, 104.

(27) Tsuji, M.; Hashimoto, M.; Nishizawa, Y.; Masatoshi, K.; Tsuji, T. *Chem. Eur. J.*, **2005**, *11*, 440.

(28) Yoshinaga, K.; Yamauchi, M.; Maruyama, D.; Mouri, E.; Koyanagi, T. *Chem. Lett.*, **2005**, *34*, 1094.

(29) Wang, D.; Liu, J.; Huo, Q.; Nie, Z.; Lu, W.; Williford, R.E.; Jiang, Y.B. *J. Am. Chem. Soc.*, **2006**, *128*, 13670.

(30) Ikeda, S.; Ikoma, Y.; Kobayashi, H.; Harada, T.; Torimoto, T.; Ohtani, B.; Matsumura, M. *Chem. Com.*, **2007**, *2007*, 3753.

(31) Matsumoto, Y.; Noguchi, M.; Matsunaga, T. *J. Phys. Chem. B*, 1999, *103*, 7190.

(32) Zhang, W.; Chen, S.; Yu, S.; Yin, Y. *J. Cryst. Growth*, **2007**, *308*, 122.

(33) Gao, Y.; Luo, H.; Mizusugi, S.; Nagai, M. *Cryst. Growth Des.*, **2008**, *8*, 1804.

(34) Ihara, T.; Miyoshi, M.; Iriyama, Y.; Matsumoto, O.; Sugihara, S. *Appl. Catal. B: Environ.*, **2003**, *42*, 403.

(35) Oliver, P.M.; Watson, G.W.; Kelsey, E.T. Parker, S.C. *J. Mater. Chem.*, **1997**, *7*, 563.

(36) Kakihana, M.; Tada, M.; Shiro, M.; Petrykin. V.; Osada, M.; Nakamura, Y. *Inorg. Chem.*, **2001**, *40*, 891.

(37) Barnard, A.S.; Zapol, P. *J. Phys. Chem. B*, **2004**, *108*, 18435.

(38) Barnard, A.S.; Curtiss, L.A. *Nono Lett.*, **2005**, *5*, 1261.

(39) Dzwigaj, S.; Arrouvel, C.; Breysse, M.; Geantet, C.; Inoue, S.; Toulhoat, H.; Raybaud, P. *J. Catal.*, **2005**, *236*, 245.

(40) Zhang, J.; Ohara, S.; Umetsu, M.; Naka, T.; Hatakeyama, Y.; Adschiri, T. *Adv. Mater.*, **2007**, *19*, 203.

(41) Ahniyaz, A.; Sakamoto, Y.; Bergström, L. *Cryst. Growth Des.*, **2008**, *8*, 1798.

(42) Wen, P.; Itoh, H.; Tang, W.; Feng, Q. *Langmuir*, **2007**, *23*, 11782.